JOM, Vol. 73, No. 11, 2021
https://doi.org/10.1007/s11837-021-04886-6




# Introducing $MnO_2$ and ZnO Additives for the Development of Alumina–Mullite–Zirconia Composites

HUDSA MAJIDIAN ,[1,2] MOHAMMAD FARVIZI,[1] and LEILA NIKZAD[1]

1.—Ceramic Department, Materials and Energy Research Center, Karaj, Alborz, Iran. 2.—e-mail: h-majidian@merc.ac.ir

Alumina-based composites have been prepared through reaction sintering of alumina and zircon. To develop these advanced composites, the effects of the addition of $MnO_2$ and ZnO (1 wt.% and 2 wt.%) on the sintering behavior, phase content, microstructure, and mechanical properties of the prepared composites were investigated. It was found that $MnO_2$ retarded the formation of mullite but increased the stability of tetragonal zirconia, whereas ZnO had the opposite effect. At 1 wt.%, both additives formed a solid solution with alumina, but using 2 wt.% resulted in the formation of a secondary phase. Both additives restricted the grain growth of alumina and hence enhanced the mechanical properties and thermal shock resistance of the composites. The results also revealed that, when using the additives, the porosity content increased slightly, but on the other hand, the formation of solid solution, refinement of grain size, stabilization of tetragonal zirconia, and increase in the mullite content were beneficial effects of these additives.

## INTRODUCTION

Alumina–mullite–zirconia (AMZ) composites are an important group of industrial ceramic composites.[1] They are commonly composed of an alumina matrix with other phases such as zirconia, mullite, or both. High strength, good thermal shock resistance, high working temperature, and excellent corrosion resistance are the main reasons for the utilization of these composites for ferrules. These composites are commonly prepared through reaction sintering of alumina and zircon. However, the porosity remaining in the final products can deteriorate the mechanical properties and restrict their applications. Also, high thermal stability is another important factor that can postpone failure.[1] Because the microstructure of these composites is highly sensitive to the porosity and microcracks,[2] the demand for high-quality ceramic parts has motived researchers to upgrade AMZ composites. The properties of alumina-based composites can be improved by appropriate design and processing. Many successful approaches have been employed to improve the properties of alumina-based composites, including milling of raw materials,[3,4] utilization of reactive materials,[5] wet colloidal processing,[6] two-step sintering,[7,8] microwave heating,[4,9] and spark plasma sintering.[10,11] One of the most beneficial approaches to enhance the physical and mechanical properties of alumina-based composites is the use of oxide additives.

The effects of oxide additives on AMZ composites have been extensively investigated; For example, MgO,[12–14] CaO,[15] $TiO_2$,[16–18] $CeO_2$,[19] and $Cr_2O_3$[20] are the most common additives used for the preparation of AMZ composites. These additives promote the densification process through the formation of liquid-phase sintering, particle rearrangement, or a diffusion mechanism.[17] $MnO_2$ and ZnO are two important oxides that can positively influence the sintering behavior and mechanical properties of ceramics such as alumina[21–28] or zirconia.[29–31] Research conducted on the effect of manganese oxide addition to alumina has shown that $MnO_2$ can promote the densification of alumina but leads to inhomogeneous grain growth.[21] However, to the best of the authors' knowledge, the effects of $MnO_2$ and ZnO addition to AMZ composites have not been investigated.

(Received March 26, 2021; accepted August 31, 2021; published online September 20, 2021)

In the work presented herein, we investigated the effects of addition of $MnO_2$ and ZnO oxides on the reaction sintering of alumina and zircon. It has been reported that $MnO_2$ is more effective for densification of alumina than other oxides such as MgO.[25] The grain boundary diffusivity of Mn is higher than that of other dopants in alumina.[22] Also, the commercial importance of alumina with manganese oxide is well reported.[21] ZnO is a desirable sintering aid that is compatible with alumina,[27] but there is a lack of information on the influence of $MnO_2$ on AMZ composites such as ferrules. Therefore, in this work, small amounts of $MnO_2$ and ZnO additives were incorporated into AMZ composites and effective parameters of the prepared composites such as densification, phase composition, microstructure, mechanical strength, and thermal shock resistance were evaluated.

## EXPERIMENTAL PROCEDURES

### Materials

Alumina (Martinswerk MR70, 0.7 $\mu$m, 99.8% purity), zircon (Global, 2.1 $\mu$m, 99.8% purity), zinc oxide (Germany, $<$ 20 $\mu$m, 99% purity), and $MnO_2$ (South Africa, $<$ 20 $\mu$m, 99% purity) powders were used as raw materials. Dolapix CE-64 (0.5 wt.%) was used as a process control agent (PCA).

### Sample Preparation and Sintering

The samples were prepared by mixing alumina and zircon powders with 0 wt.%, 1 wt.%, and 2 wt.% of additive oxides in the presence of 0.5 wt.% of Dolapix dissolved in water using a planetary mill (250 rpm) for 3 h. Previous studies[7] have shown that AMZ composites with an alumina-to-zircon weight ratio of 85/15 exhibit better properties. Therefore, in the current study, this ratio was selected for the preparation of samples. After ball milling, the mixtures were dried using a magnetic heater, then granulated by passing through 60 mesh and 100 mesh sieves. Granules were pressed uniaxially at 250 MPa. Green samples were sintered at 1650°C with holding time of 3 h. The sintering atmosphere was air, and after the sintering procedure, samples were furnaced cooled. Sintered samples were coded as presented in Table I.

### Characterization

The apparent porosity of the sintered samples was determined using the standard water adsorption method (ASTM C20). At least three samples were tested to obtain a mean value for each test. Crystalline phases in sintered samples were characterized by x-ray diffraction (XRD) analysis (Siemens, D500 system) using Cu $K_\alpha$ radiation at an accelerating voltage of 30 kV. Moreover, quantitative analysis of the prepared samples was performed using the Rietveld refinement technique with Material Analysis Using Diffraction (MAUD) software, which applies the least-squares method. Instrumental broadening was removed using a defect-free silicon sample. In all refinements, Sig. and $R$ values were less than 2 and 10, respectively. The microstructure of the sintered samples was studied by scanning electron microscopy (SEM, VEGA II SCAN) on polished and thermally etched (at 150°C below the sintering temperature for 20 min) surfaces. The grain size of samples was estimated by using ImageJ analysis software. The sizes of individual grains were measured, a method that can be reliable and avoids accounting for attached grains or phase particles. About five SEM micrographs including up to 100 measurements were evaluated. Thermal shock resistance was measured according to the loss of mechanical strength after 20 min of oven heating at 300°C and 600°C followed by quenching in air.[7] Five samples with dimensions of 5 mm × 6 mm × 25 mm were used for used for each mechanical strength test.

## RESULTS AND DISCUSSION

### Phase Composition of Composite A0

According to the XRD pattern of sample A0, monoclinic zirconia (Zm), tetragonal zirconia (Zt), and mullite (M) were the main phases dispersed in the alumina (A) matrix. To investigate the reaction sintering between alumina and zircon, the resulting phases of this reaction (mullite and zirconia) must be evaluated. The main peak of mullite is located at $2\theta = 26°$ (Fig. 1a). According to the results of the refinement process (Fig. 2), the content of mullite in composite A0 was insignificant (2.9 wt.%). The

**Table I. Sample codes for the sintered composites**

| Sample code | Composition (wt.%) | Additive (wt.%) |
|---|---|---|
| A0 | 85% alumina + 15% zircon | – |
| AM1 | 85% alumina + 15% zircon | 1% $MnO_2$ |
| AM2 | 85% alumina + 15% zircon | 2% $MnO_2$ |
| AZ1 | 85% alumina + 15% zircon | 1% ZnO |
| AZ2 | 85% alumina + 15% zircon | 2% ZnO |

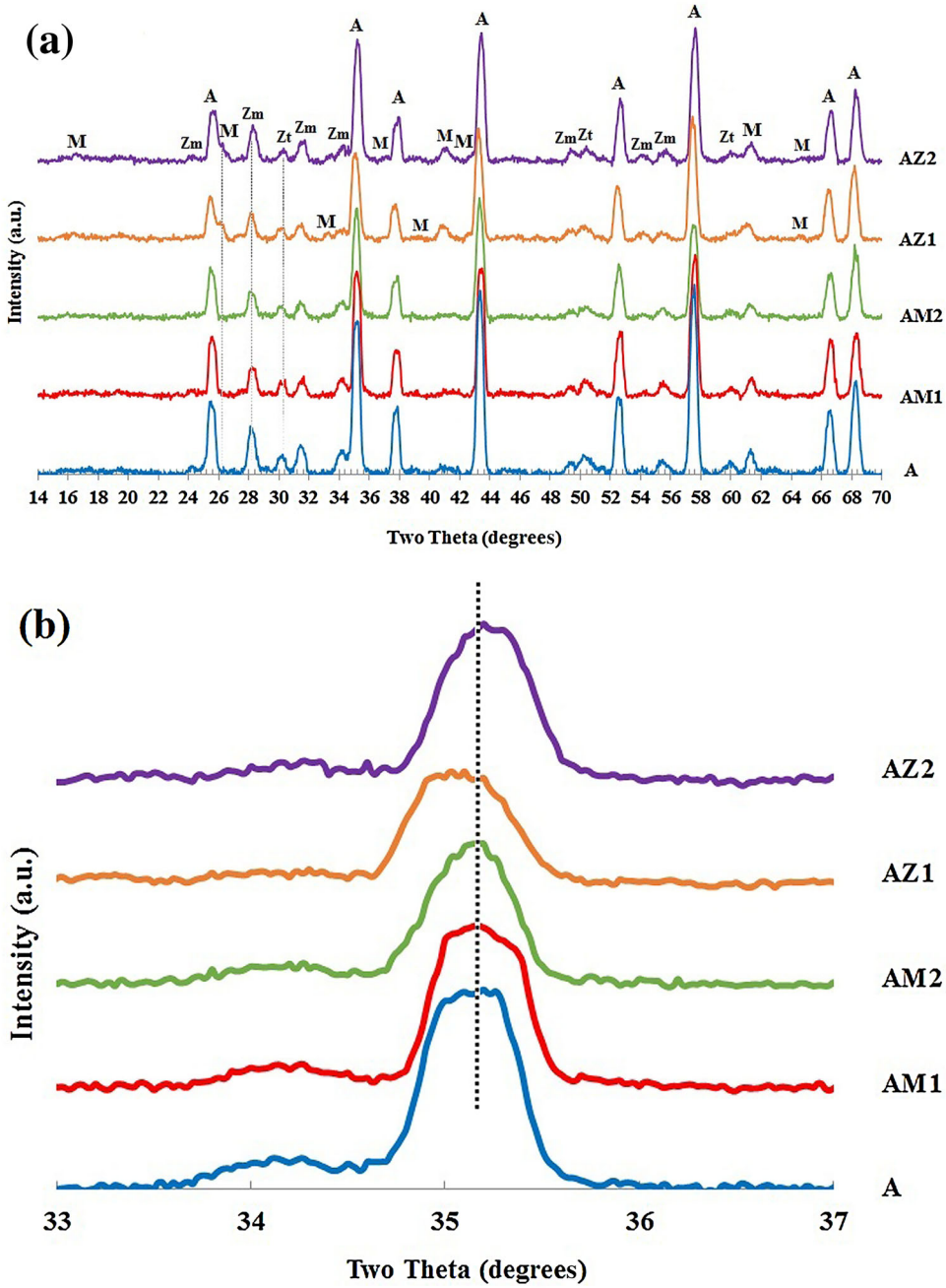


Fig. 1. XRD patterns of prepared composites in two different ranges (a) $2\theta$ = 20° to 70° and (b) $2\theta$ = 33° to 37°. A, alumina; M, mullite; Zm, monoclinic zirconia, Zt, tetragonal zirconia.

peaks at $2\theta$ = 28° and $2\theta$ = 30° confirmed the presence of monoclinic (18.5 wt.%) and tetragonal (7.6 wt.%) zirconia phases, respectively. The presence of zirconia and mullite phases indicates dissociation of zircon and the occurrence of reaction sintering, respectively. The formation of a large amount of zirconia with a low content of mullite in composite A0 shows that dissociation of zircon occurred but the reaction sintering was incomplete. The presence of Zt in composite A0 confirms that part of the zirconia can be stabilized without any additive. Previous studies[32] have shown that small tetragonal zirconia does not transform to the monoclinic phase.

Figure 1 shows the XRD results for the prepared AMZ composites in two different ranges. The weight percentages of different phases were calculated by the Rietveld refinement method (Fig. 2).

## Effect of $MnO_2$ Addition on Phase Constituents of AMZ Composites

According to the XRD patterns of samples AM1 and AM2, it was found that the main peak of mullite

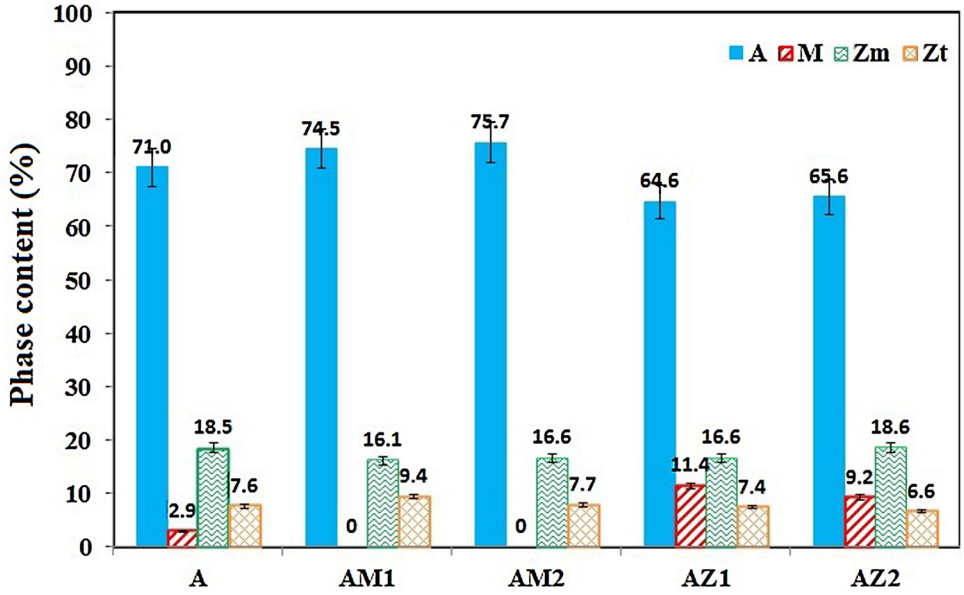


Fig. 2. Phase content of prepared composites obtained from Rietveld refinement analysis.

at $2\theta = 26°$ could not be observed with addition of 1 wt.% and 2 wt.% $MnO_2$ to AMZ composites. The observation of zirconia peaks shows that the zircon dissociated into zirconia and silica, but the reaction between silica and alumina was incomplete. Comparison of the phase contents of samples AM1 and AM2 samples with sample A0 reveals that the alumina content in the $MnO_2$-doped samples was higher than composite A0. The reason for this phenomenon is not known.

Amorphous silica formed after dissociation of zircon can react with Mn to form a new phase. $MnAl_2O_4$ ($2\theta = 66.7°$), $MnSiO_3$ ($2\theta = 34°$), and $Mn_2SiO_4$ ($2\theta = 35.1°$) are the common compounds in the $MnO–SiO_2–Al_2O_3$ system.[33,34] These are low-melting phases that may be formed at the sintering temperature.[35] It was supposed that Mn silicate amorphous phases are more likely to exist than $MnAl_2O_4$. This idea is supported by the fact that the Gibbs free energies of manganese silicates (about –800 kJ/mol to –2200 kJ/mol)[36] are lower than that of $MnAl_2O_4$ (about –34 kJ/mol)[37] at the sintering temperature. In this study, the amount of $MnO_2$ was low and peaks related to the probable secondary phases were not observed. Also, the XRD peaks of these phases can overlap with alumina and Zm peaks. Formation of $MnAl_2O_4$ spinel or the solid solution of Mn in alumina has been reported by other researchers,[21,25] but this hypothesis could not be confirmed by the corrsponding XRD patterns in our study.

Formation of a substitutional solid solution can increase the stress level in alumina, which can lead to a shift in its peaks.[38] Figure 1b reveals that no shift in the main peak of alumina in samples AM1 and AM2. This can be interpreted based on the similar ionic radii of $Al^{3+}$ (51 pm) and $Mn^{4+}$ (53 pm). Also, Farag et al.[39] concluded that manganese ions may enter the alumina lattice as $Mn^{3+}$. $Mn^{3+}$ has the same valency and ionic radius as $Al^{3+}$. Hence, a certain amount of $Mn^{3+}$ dissolves in the alumina lattice but does not result in lattice defects or a detectable change of the alumina lattice parameters.

Figure 2 also shows that the total amount of zirconia decreased. The inhibition effect of $MnO_2$ on zircon dissociation was investigated in our previous study.[40] The Rietveld refinement results (Fig. 2) show that, with addition of $MnO_2$, the weight percentage of Zm reduced slightly. On the other hand, addition of 1 wt.% $MnO_2$ led to an increment in the Zt content. This means that addition of 1 wt.% $MnO_2$ had a stabilizing effect on Zt. Such stabilization of Zt by manganese oxide was discussed previously.[40] The lower content of Zt in composite AM2 can be attributed to the fact that Mn was consumed in the formation of new phases and further increase of the additive did not result in stabilization of Zt.

## Effect of ZnO Addition on Phase Constituents of AMZ Composites

As seen in Figs. 1 and 2, the content of mullite phase was enhanced considerably after addition of 1 wt.% and 2 wt.% ZnO to the AMZ composites. For example, sample AZ1 contained 11.4 wt.% while sample AZ2 included 9.2 wt.% mullite, indicating a promotion of the formation of mullite. This increase corresponds to the decrease of the alumina content in the AZ samples. This means that more reaction sintering between alumina and zircon occurred in the presence of ZnO particles.

$Zn_2SiO_4$ ($2\theta = 31.8°$) is the likely binary compound in the $ZnO–SiO_2$ system.[41,42] Also, $ZnAl_2O_4$, ($2\theta =$

36.9°)[27,43,44] is a common compound that can be observed in this system.

The Rietveld refinement results (Fig. 2) showed that the total amount of zirconia was decreased by addition of 1 wt.% ZnO and that further increase of the ZnO content to 2 wt.% resulted in a slight increase of zirconia. The decrease in the amount of Zt in the AZ samples implies that ZnO cannot stabilize tetragonal zirconia anymore. This can be related to the consumption of ZnO in the formation of a new phase.

Figure 1b shows a slight shift in the alumina peak at $2\theta$ = 35.1° to smaller angles for sample AZ1. This means that a solid solution of Zn in alumina may be formed. The shift of the alumina peak to lower angles can be interpreted based on the larger ionic radius of $Zn^{2+}$ (74 pm) compared with $Al^{3+}$ (51 pm). Deformation of the alumina structure with ZnO dopant has been reported.[28] This shift was not observed for sample AZ2. Maybe, Zn has low solubility in alumina and 2 wt.% ZnO lies beyond this solubility limit.

Figure 1b also shows that the alumina peak of sample AZ2 at $2\theta$ = 35.1° was broadened slightly compared with sample A0. The broadening of this XRD peak is related to the formation of the secondary phase and its grain boundary pinning effect.[15]

## Microstructural Study of Composite A0

SEM micrographs of the prepared samples and the image analysis results are shown in Fig. 3 and Supplementary Fig. S1, respectively. Figure 4 shows the SEM-EDS analysis taken from grain boundaries of samples AM2 and AZ2. EDS mapping analysis of the evolved phases of samples A0, AM2, and AZ2 is shown in Fig. 5.

As seen in Figs. 3a and 5a, the grey matrix is alumina (labeled as A) and white grains are related to the zirconia phase. The zirconia grains are mainly intergranular and irregular. Two types of zirconia grain can be detected in this figure: intragranular spherical zirconia within the grains of the matrix, and intergranular zirconia between grains. Microstructural studies of this sample also confirmed the existence of minor fractions of fine zirconia, mullite, and glassy phase.

Some pores and fine microcracks were observed in the microstructure. The formation of porosities in sample A0 indicates that the densification was not complete in this sample.

## Effect of $MnO_2$ on Microstructure of AMZ Composites

Addition of 1 wt.% manganese oxide did not cause a dramatic change in the microstructure (Fig. 3b). Sample AM2 contained more rounded grains, which can be attributed to the presence of the glassy phase (Fig. 3c). The glassy phase can facilitate grain rearrangement and, therefore, leads to the formation of a homogeneous microstructure. The existence of the Mn-rich glassy phase at grain boundaries of sample AM2 was hard to detect (Fig. 4a). EDS analysis taken from the grain boundary of sample AM2 shows strong peaks of Mn and Si (Fig. 4c), suggesting the formation of the manganese silicate phase.

EDS mapping analysis of sample AM2 showed Mn dispersed throughout the composite, providing evidence for the formation of solid solution (Fig. 5b). Also, Mn was present at the grain boundaries accompanied by Si, thus as anticipated in Sect. 3.1.2, it can be concluded that Mn could substitute at Al sites up to its solubility limit while extra Mn was incorporated through the formation of a secondary phase (manganese silicate phase) at grain boundaries. An additive can form a solid solution or can function as a secondary phase, or show both effects.[18] Excess additive (beyond the solubility limit) forms secondary phases or segregate from the grains.[38]

## Effect of ZnO on Microstructure

According to Fig. 3d and e, addition of 1 wt.% ZnO did not affect the microstructure, but addition of 2 wt.% ZnO changed the microstructure dramatically. More rounded and smooth grains are seen in sample AZ2. This rounded grain morphology is due to the presence of the glassy phase,[14,23] which is retained mostly at triple junctions. The high content of glassy phase in the AZ composites could be a reason for their high mullite content (Fig. 2). A higher amount of glassy phase means more melt in the microstructure, thus the dissolution of the alumina in silica glassy phase is easier, which promotes formation of mullite.[12] Investigation of the grain structure in Fig. 4b shows that two types of grain exist in the microstructure. The large grains correspond to alumina, while the small grains (around the large ones and at grain boundaries) can be attributed to the secondary phase ($Zn_2SiO_4$) or melted zinc spinel ($ZnAl_2O_4$). It has been reported that $ZnAl_2O_4$ spinel melts at 1600°C and produces a glassy phase;[27] therefore, ZnO additive can promote sintering of alumina through the liquid-phase sintering mechanism. This can be the reason for the high amount of glassy phase observed in the AZ composites. The coarsening of grain boundaries in composite AZ2 occurred due to segregation of the additive, as also reported by other researchers in ZnO-doped alumina.[28]

Figure 4d shows that Zn, Al, and Si elements were present at grain boundaries. EDS mapping analysis of composite AZ2 showed that Zn was highly dispersed in both the alumina matrix and zirconia grains. These results thus support the idea of a reaction between Zn and alumina to form zinc aluminate rather than zinc silicate. However, Mn and Zn did not segregate at the grain boundaries

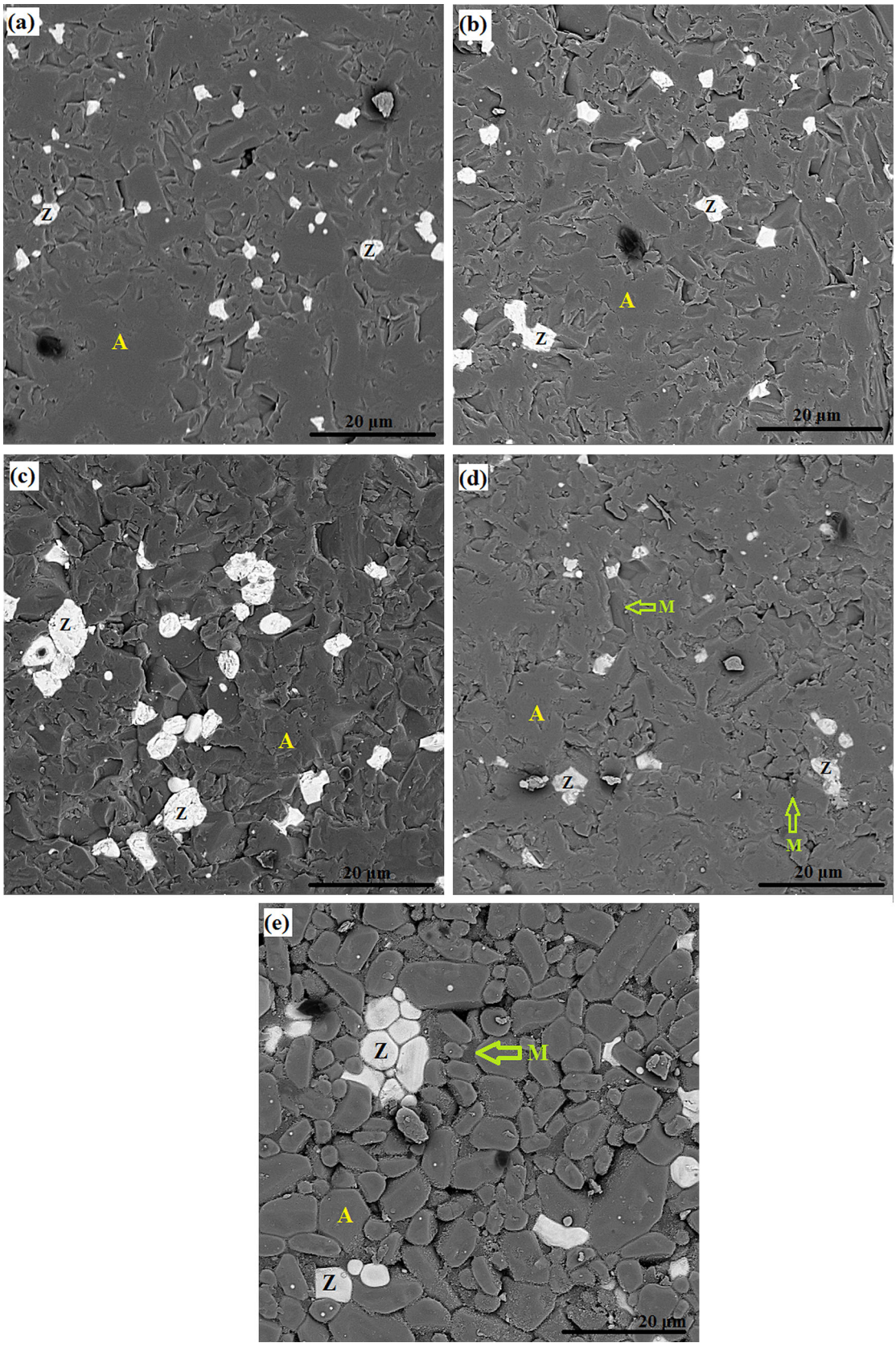


Fig. 3. SEM micrographs of prepared composites: (a) A0, (b) AM1, (c) AM2, (d) AZ1, and (e) AZ2.

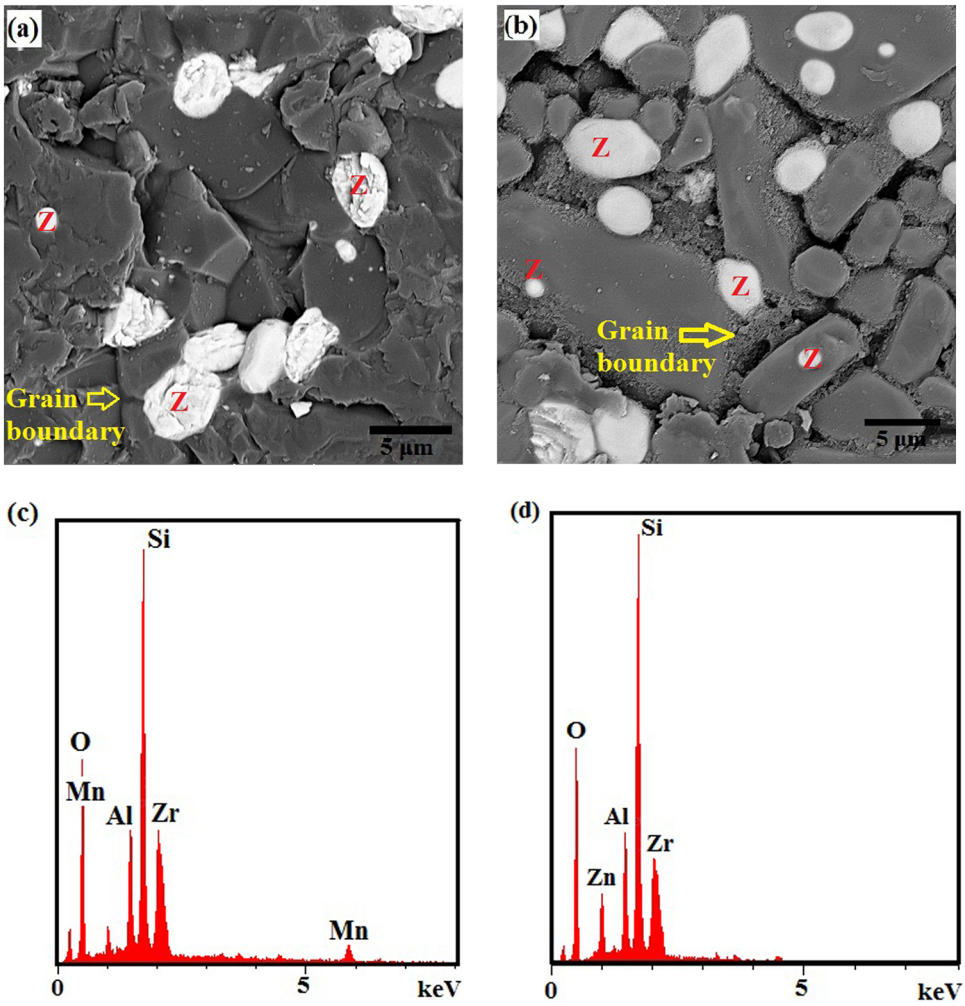


Fig. 4. SEM-EDS analysis taken from grain boundary of composites (a, c) AM2 and (b, d) AZ2.

along with Si. This suggests that Mn has greater affinity to react with silica compared with Zn.

## Grain Size of Prepared Composites

The average grain size of the alumina and zirconia grains is presented in Table II. The results show that $MnO_2$ and ZnO addition did not result in alumina grain growth. In fact, addition of 2 wt.% ZnO resulted in the minimum grain size in the prepared AMZ composites (6.2 $\mu$m for composite AZ2). It was supposed that grain boundary migration was restricted by the secondary phase formed at the grain boundaries due to its pinning effect. The manganese silicate phase and $ZnAl_2O_4$ spinel act as barriers to the diffusion of boundaries and hindered alumina grain growth. Higher grain size of the zirconia phase was observed for all the composites. This growth occurs because the mentioned additives improve zircon dissociation. More zircon dissociation leads to more zirconia phase, which can aggrefate to form large zirconia grains.[15]

## Mechanical Properties of Composite A0

Table III presents the physical and mechanical properties of the prepared composites. The composite sample processed without additive (sample A0) showed a porosity of about 1.8%. The porosity of the prepared composites generally increased with incorporation of additives. The porosity remaining in the AMZ composites can be attributed to: (1) formation of secondary phase and inhibition of ion migration, (2) promotion of the reaction sintering process between alumina and zircon, which increases the porosity content, and (3) the lower density of the products (mullite) compared with the raw materials.

## Effect of $MnO_2$ on Mechanical Properties

Addition of 1 wt.% manganese oxide led to a slight decrease in the porosity (1.4%) but an increase in the density (3.26 g/cm$^3$) of AMZ. The density increase can be related to the elimination of the low-density mullite phase (3.2 g/cm$^3$) in the products. Also, the formation of the solid solution of Mn

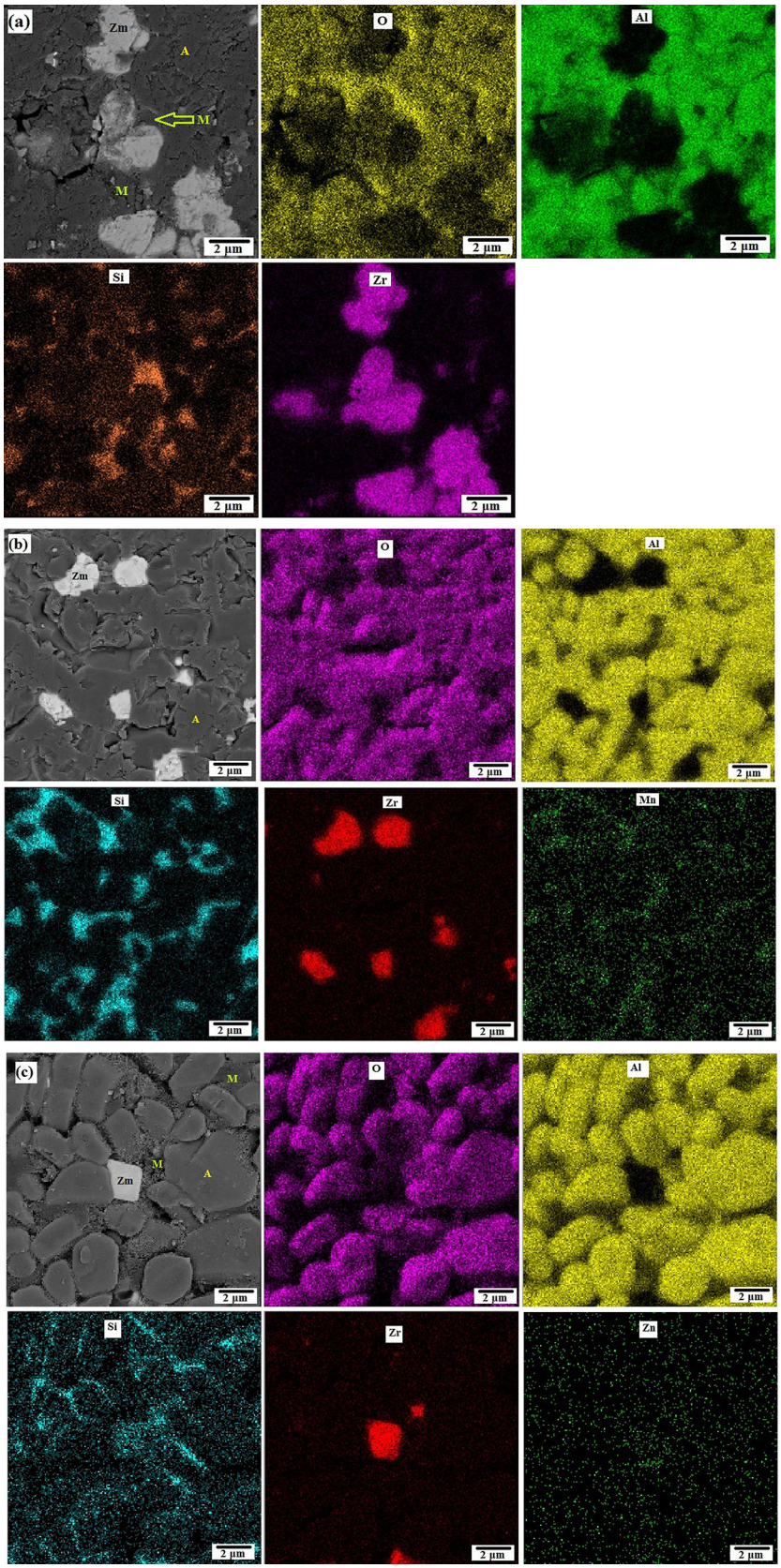


Fig. 5. EDS mapping analysis of composites (a) A0, (b) AM2, and (c) AZ2.

**Table II. Average grain size of alumina (±4 μm) and zirconia grains (±2 μm) in the AMZ composites**

| Composite | Grain size of alumina (μm) | Grain size of monoclinic zirconia (μm) |
|---|---|---|
| A0 | 10.6 | 2.5 |
| AM1 | 10.1 | 3.1 |
| AM2 | 8.4 | 4.4 |
| AZ1 | 9.0 | 2.7 |
| AZ2 | 6.2 | 4.5 |

**Table III. Physical and mechanical properties of prepared composites**

| Composite | Density ($g/cm^3$) | Porosity (%) | MOR at RT (MPa) | MOR after 300°C Thermal Shock (MPa) | MOR after 600°C Thermal Shock (MPa) | Loss of MOR (%) |
|---|---|---|---|---|---|---|
| A0 | 3.11 ± 0.05 | 1.8 ± 0.3 | 170 ± 22 | 85 ± 25 | 80 ± 27 | 53 |
| AM1 | 3.26 ± 0.03 | 1.4 ± 0.2 | 191 ± 18 | 175 ± 22 | 149 ± 26 | 22 |
| AM2 | 2.93 ± 0.05 | 2.7 ± 0.3 | 225 ± 20 | 192 ± 23 | 156 ± 24 | 30 |
| AZ1 | 3.50 ± 0.04 | 2.4 ± 0.2 | 209 ± 16 | 171 ± 20 | 150 ± 22 | 28 |
| AZ2 | 3.48 ± 0.03 | 3.7 ± 0.2 | 231 ± 15 | 171 ± 19 | 168 ± 23 | 27 |

in alumina was beneficial for the densification, because the formation of a solid solution results in close bonding between grains.[45] Therefore, the 1 wt.% manganese oxide can act as a sintering aid. The enhanced grain boundary diffusion leads to better densification.[18]

Further addition of $MnO_2$ (2 wt.%) had the oppposite effect (2.7% porosity and 2.93 $g/cm^3$ density). There are various reasons for the increase of the porosity of Mn-doped alumina bodies (beyond a certain amount of Mn): (1) retention of closed pores in alumina grains,[46] (2) formation of cracks due to addition of manganese oxide,[23] and (3) formation of a secondary phase.[18,21,38,47] Secondary phases can block the movement of grain boundaries and hinder densification.

Composites AM1 and AM2 both showed higher mechanical strength (modulus of rupture, MOR) compared with composite A0 (170 MPa). The higher MOR of composite AM1 (191 MPa) can be attributed to its enhanced densification and the formation of a solid solution. Also, composites with more Zt phase showed higher mechanical strength. It has been shown that the polymorphic change of Zt to Zm causes microcracks that degrade the mechanical strength.[32,38]

Although it is known that porosity degrades mechanical strength, the improvement of the mechanical strength of AM2 composite (225 MPa) can be attributed to the formation of a solid solution and the evolution of a finer microstructure. Composite AM2 showed a smaller alumina grain size compared with composite A0.

## Effect of ZnO on Mechanical Properties

ZnO is known to act as a sintering aid that improves alumina densification through: (1) decreasing pore diameter,[26,27] (2) coarsening of grain boundaries, which facilitates ion migration, and (3) increasing the formation of the liquid phase. On the other hand, it was believed that migration of grain boundaries can be restricted by the formation of secondary phases located at grain boundaries, thus hindering densification too.[26] The porosity of composites AZ1 (2.4%) and AZ2 (3.7%) were higher than that of composite A0; Samples AZ1 and AZ2 also showed higher densities (3.50 $g/cm^3$ and 3.55 $g/cm^3$, respectively). Formation of $ZnAl_2O_4$ spinel phase occurred before densification of alumina.[44] The volume changes during the formation of this new phase accompained by mullite formation can produce pores in the microstructure.

It is of interest that the mechanical strength of the composites was also increased by addition of ZnO. The improvement of the mechanical strength of 2 wt.% ZnO-doped alumina can be interpreted[27,28] as being due to the refinement of the grain size, good dispersion of ZnO in alumina matrix, and formation of the secondary phase. Solid-solution strengthening has also been mentioned as a reason for the improvement of mechanical properties. In addition to these facts, composites AZ1 and AZ2 have also higher mullite content; completion of the solid-state reaction (mullite formation) is the other reason for the improvement of the MOR value.[13]

## Thermal Shock Resistance of Prepared AMZ Composites

Table III also presents the decrease of the MOR of the prepared composites after thermal shock tests at 300°C and 600°C. The loss of MOR of composites AM1 and AM2 was 22% and 30%, which is better than the result for composite A0 (53%). This means that addition of manganese oxide increases the thermal shock resistance of AMZ composites. AZ

composites also showed better thermal shock resistance than composite A0. This improvement of the thermal shock resistance can be attributed to the enhanced mechanical strength and porosity remaining in the microstructure.[7] Zm and Zt are both beneficial for the thermal shock resistance of a composite through microcrack or transformation mechanisms, respectively. Higher mullite content of AZ composites can also enhanced the thermal shock resistance[7] as mullite has a lower thermal expansion coefficient ($4 \times 10^{-6}$/°C to $5 \times 10^{-6}$/°C) compared with alumina ($7.5 \times 10^{-6}$/°C to $8.5 \times 10^{-6}$/°C).

## CONCLUSION

Alumina–mullite–zirconia composites were prepared through reaction sintering of alumina and zircon powders. $MnO_2$ and ZnO (1 wt.% and 2 wt.%) were added to the composites, and their effects on the sintering behavior, phase content, formation of solid solution, microstructure, and mechanical properties of the prepared composites investigated. The results revealed that $MnO_2$ retarded the formation of mullite. However, the reaction of ZnO with alumina resulted in acceleration of the formation of mullite. $MnO_2$ was beneficial for stabilization of tetragonal zirconia. Both additives formed a solid solution with alumina at 1 wt.%, but with further addition up to 2 wt.%, formation of a secondary phase was observed. The secondary phase was probably manganese silicate (on addition of $MnO_2$) or zinc aluminate (on addition of ZnO) according to microstructural observations. Grain growth of alumina was restricted by incorporation of these additives. The results also revealed that, although the porosity was increased slightly, the formation of solid solution, refinement of grain size, stabilization of tetragonal zirconia, and increase of the mullite content were beneficial effects of these additives, thereby improving the mechanical properties and thermal shock resistance of the composites.

## ACKNOWLEDGEMENTS

This study was carried out under the financial support of the Iran National Science Foundation (INSF-96008505).

## CONFLICT OF INTEREST

The authors declare that they have no conflicts of interest.

## SUPPLEMENTARY INFORMATION

The online version contains supplementary material available at https://doi.org/10.1007/s11837-021-04886-6.

## REFERENCES

1. G. Quercia, Y. Perera, H. Tovar, and E. Rodríguez, *Acta Microsc.* 16, 205. (2007).
2. C.R. Ferrari, and J.A. Rodrigues, *Bol. Soc. Esp. Ceram. Vidrio* 42, 15. (2003).
3. R. Zamani Foroushani, R. Emadi, and H. Ashrafi, *Ceram. Silik.* 59, 216. (2015).
4. O. Ertugrul, R. Dalmis, S. Akpinar, I.M. Kusoglu, and E. Celik, *Ceram. Int.* 42, 11104. (2016).
5. H. Majidian, L. Nikzad, H.E. Shahed, and T. Ebadzadeh, *Int. J. Appl. Ceram. Technol.* 13, 1024. (2016).
6. A. Khorsand, H. Majidian, and M. Farvizi, *Int. J. Appl. Ceram. Technol.* 17, 1822. (2020).
7. H. Majidian, T. Ebadzadeh, and E. Salahi, *Mater. Sci. Eng. A.* 530, 585. (2011).
8. H. Majidian, T. Ebadzadeh, and E. Salahi, *Ceram. Int.* 36, 1669. (2010).
9. H. Majidian, L. Nikzad, H.E. Shahed, and T. Ebadzadeh, *Int. J. Mater. Res.* 106, 1269. (2015).
10. M.C. Anjali, P. Biswas, D. Chakravarty, U.S. Hareesh, Y.S. Rao, and R. Johnson, *Sci. Sintering* 44, 323. (2012).
11. E.R. Rangel, S.D. Torre, M. Umemoto, H. Miyamoto, and H.B. Ramirez, *J. Am. Ceram. Soc.* 88, 1150. (2005).
12. S. Abdolazizi, R. Naghizadeh, and S. Baghshahi, *ACERP* 1, 11. (2015).
13. M.M.S. Wahsh, R.M. Khattab, and M. Awaad, *Mater. Des.* 41, 31. (2012).
14. S. Maitra, S. Pal, S. Nath, A. Pandey, and R. Lodha, *Ceram. Int.* 28, 819. (2002).
15. D. Chandra, G. Das, and S. Maitra, *Int. J. Appl. Ceram. Technol.* 124, 771. (2015).
16. A.S. Khamneh, and D. Rasouli, *Am. J. Mater. Res.* 4, 27. (2017).
17. M. Sathiyakumar, and F.D. Gnanam, *Ceram. Int.* 28, 195. (2002).
18. H. Erkalfa, Z. Misirli, and T. Baykara, *Ceram. Int.* 24, 81. (1998).
19. J.S. Wang, J.F. Tsai, D.K. Shetty, and A.V. Virkar, *J. Mater. Res.* 5, 1948. (1990).
20. M. Kuntz, and R. Krüger, *Ceram. Int.* 44, 2011. (2018).
21. H. Erkalfa, Z. Misirli, M. Demirci, C. Toy, and T. Bayha, *J. Europ. Ceram. Soc.* 15, 165. (1995).
22. M. Nagashima, K. Motoike, and M. Hayakawa, *J. Ceram. Soc. Jpn.* 116, 645. (2008).
23. I.H. Bang, K.O. Kim, and S.J. Lee, *J. Ceram. Process. Res.* 15, 525. (2014).
24. J. Kim, J.H. Ha, J. Lee, and I.H. Song, *J. Korean Ceram. Soc.* 54, 331. (2017).
25. C. Chuen Rong, Bachelor of Engineering project report, University Tunku Abdul Rahman (2011).
26. T. Alam, K.H.A. Al Mahmuda, M.F. Hasan, S.A. Shahir, H.H. Masjuki, M.A. Kalam, A. Imran, and H.M. Mobarak, *Procedia Eng.* 68, 723. (2013).
27. H. Bouhamed, and S. Baklouti, *Powder Technol.* 264, 278. (2014).
28. N. Mehalawy, M. Awaad, T. Eliyan, M.A. Abd Allah, and S.M. Naga, *J. Mater. Sci. Mater. Electron.* 29, 13526. (2018).
29. D. Ragurajan, M. Satgunam, M. Golieskardi, A.K. Ariffin, and M.J. Ghazali, *J. Aust. Ceram. Soc.* 52, 128. (2016).
30. J. Stępień, M. Sikora, C. Kapusta, D. Pomykalska, and M.M. Bućko, *J. Appl. Phys.* 123, 185108. (2018).
31. J. Wang, G. Li, Z. Li, C. Tang, Z. Feng, H. An, H. Liu, T. Liu, and C. Li, *Sci. Adv.* 3, 1. (2017).
32. M. Rahmani, K. Jangorban, and S. Otroj, *Ceram. Silik.* 56, 215. (2012).
33. K.T. Jacob, Canadian. *J. Metall. Mater. Sci.* 20, 189. (1981).
34. I. Jung, Y. Kang, S.A. Decterov, and A.D. Pelton, *Metall. Mater. Trans. B* 35B, 259. (2004).
35. D. Kim, K. Han, B. Lee, I. Han, J. Park, and C. Lee, *Metall. Mater. Trans. A* 45A, 2046. (2014).
36. J.H. Huang, and E. Rosén, *Phys. Chem. Miner.* 21, 228. (1994).
37. L. Kong, Z. Deng, and M. Zhu, *ISIJ Int.* 57, 1537. (2017).

38. N.A. Rejab, A.Z. Ahmad Azhar, M.M. Ratnam, and Z.A. Ahmad, *Int. J. Refract. Met. Hard Mater.* 41, 522. (2013).
39. I.S.A. Farag, M.F. Kotkata, M.M. Selim, I.K. Battisha, and M.M. El- Rafaay, Egypt. *J. Solids* 27, 233. (2004).
40. H. Majidian, L. Nikzad, and M. Farvizi, *JOM* 72, 4042. (2020).
41. R. Hansson, B. Zhao, P.C. Haye, and E. Jak, *Metall. Mater. Trans. B* 36B, 187. (2005).
42. I. Isomaki, R. Zhand, L. Xia, N. Hellsten, and P.A. Taskinen, *Trans. Nonferrous Met. Soc. China* 28, 1869. (2018).
43. N. Tanaka, T. Iseki, L. Ling, R. Shimpo, and O. Ogawa, *Shigen-to-Sozai.* 114, 567. (1998).
44. K.T. Jacob, *Thermochim. Acta* 15, 79. (1976).
45. J. Liu, Z. Wang, X. Wang, H. Liu, and Y. Ma, *Int J. Ceram. Eng. Sci.* 1, 51. (2019).
46. C. Toy, M. Demirci, S. Onurlu, M. Sadik Tasar, and T. Baykara, *J. Mater. Sci.* 30, 4183. (1995).
47. H. Erkalfa, Z. Misirli, and T. Baykara, *Ceram. Int.* 21, 345. (1995).